

# Age-related changes in the energy of human mesenchymal stem cells

Mario Barilani<sup>1</sup>  | Christopher Lovejoy<sup>2</sup> | Roberta Piras<sup>1</sup> |  
Andrey Y. Abramov<sup>3</sup>  | Lorenza Lazzari<sup>1</sup> | Plamena R. Angelova<sup>3</sup>

<sup>1</sup>Department of Transfusion Medicine and Hematology, Laboratory of Regenerative Medicine – Cell Factory, Fondazione IRCCS Cà Granda Ospedale Maggiore Policlinico, Milano, Italy

<sup>2</sup>Department of Neurodegenerative Disease, UCL Queen Square Institute of Neurology, London, UK

<sup>3</sup>Department of Clinical and Movement Neurosciences, UCL Queen Square Institute of Neurology, London, UK

## Correspondence

Plamena R. Angelova, Department of Clinical and Movement Neurosciences, UCL Queen Square Institute of Neurology, Queen Sq, London WC1N 3BG, UK.  
Email: [p.stroh@ucl.ac.uk](mailto:p.stroh@ucl.ac.uk)

## Funding information

Engineering and Physical Sciences Research Council (EPSRC), Grant/Award Number: EP/R024898/1

## Abstract

Aging is a physiological process that leads to a higher risk for the most devastating diseases. There are a number of theories of human aging proposed, and many of them are directly or indirectly linked to mitochondria. Here, we used mesenchymal stem cells (MSCs) from young and older donors to study age-related changes in mitochondrial metabolism. We have found that aging in MSCs is associated with a decrease in mitochondrial membrane potential and lower NADH levels in mitochondria. Mitochondrial DNA content is higher in aged MSCs, but the overall mitochondrial mass is decreased due to increased rates of mitophagy. Despite the higher level of ATP in aged cells, a higher rate of ATP consumption renders them more vulnerable to energy deprivation compared to younger cells. Changes in mitochondrial metabolism in aged MSCs activate the overproduction of reactive oxygen species in mitochondria which is compensated by a higher level of the endogenous antioxidant glutathione. Thus, energy metabolism and redox state are the drivers for the aging of MSCs/mesenchymal stromal cells.

## KEYWORDS

aging, bioenergetics, bone marrow, cellular senescence, mitochondria, MSC

## 1 | INTRODUCTION

Progress in medicine increased the life expectancy in most of the countries around the world. Consequently, the proportion of the aged versus young people in society has been steadily augmenting. This brought age-related problems to the front line (Cylus et al., 2019). Aging is a physiological process occurring over life that induces a general decline of physical and mental capacities. Human aging leads to a higher risk for individuals to develop cancer, neurodegenerative, cardiovascular, and metabolic disorders (Kennedy et al., 2014). Therefore, a better understanding of the biological

pathways associated with aging would contribute to the improvement of the quality of life of the elderly. Yet, researchers in the field defined hallmarks of aging to foster the comprehension of this process. Among them, stem cell exhaustion was indicated as the cause of impaired regeneration of injured organs and loss of tissue homeostasis. Furthermore, other theories of aging were proposed, including genetic predisposition, programmed senescence, DNA damage, endocrine dysfunction, or the free radical hypothesis (Angelova & Abramov, 2016; Lopez-Otin et al., 2013). Most of these hypotheses are linked to cellular organelles named mitochondria, which play a role of an energy plant and are also responsible for other

Lorenza Lazzari and Plamena R. Angelova are senior authors.

This is an open access article under the terms of the Creative Commons Attribution-NonCommercial-NoDerivs License, which permits use and distribution in any medium, provided the original work is properly cited, the use is non-commercial and no modifications or adaptations are made.

© 2021 The Authors. *Journal of Cellular Physiology* published by Wiley Periodicals LLC

vital functions in the eukaryotic cell, including control of the process of cell death and free radical production. However, the main function of mitochondria is producing energy in the form of ATP and all other processes inside of mitochondria are connected or dependent on bioenergetics.

In this frame, adult tissue-specific stem cells represent a suitable cell type to study age-related changes in bioenergetics. Specifically, mesenchymal stem/mesenchymal stromal cells (MSC) from bone marrow are a relevant and crucial model to study aging for several reasons: a) access to cells of individuals with different age, which allows for the study of chronological aging rather than replicative senescence (Demirovic et al., 2015; Ganguly et al., 2017; Geissler et al., 2012; Y. K. Yang, 2018), even in the case of fetal sources (Barilani, Palorini, et al., 2019; Gu et al., 2016); b) influence of aging on properties and functionality of bone marrow niche cells (Hoffman et al., 2019), already extensively documented by others for what concerns proliferation and differentiation (Beane et al., 2014; Ganguly et al., 2019; Kretlow et al., 2008; Lund et al., 2010; Stolzing et al., 2008; Zaim et al., 2012); c) use of MSC in diverse clinical applications, such as bone reconstruction (Gómez-Barrena et al., 2020); and d) lack of information regarding age-related bioenergetics changes for MSC participating in programs of tissue regeneration. Indeed, metabolism is a growing area of research in the stem cell field, as the influence of mechanisms of energy production on stem cell physiology and disease is increasingly recognized. In particular, metabolism and mitochondria themselves have been associated with stem cell self-renewal, cell fate decisions, and differentiation control (Shyh-Chang et al., 2013). Finally, in addition to canonical paracrine and differentiation mechanisms of action of MSC, a new one also involved in bone marrow niche homeostasis and therapeutic efficacy has been recently ascribed to horizontal transfer of mitochondria to damaged cells (Ahmad et al., 2014; Cho et al., 2012; Han et al., 2016; Hsu et al., 2016; Spees et al., 2006; Théry et al., 2018; Torralba et al., 2016). Yet, envisioning a "mitotherapy" scenario using MSC, the selection of the best mitochondrial donor would be pivotal to attain optimal rescue of the dysfunctional phenotype. Here, we found that aged MSC has a lower rate of glucose metabolism and decreased mitochondrial membrane potential and mitochondrial NADH redox state. Aged MSC exhibits overall lower net mitochondrial mass, despite higher mitochondrial DNA (mtDNA) content, due to increased rates of mitophagy. Finally, because of higher rates of ATP consumption, aged MSC is more vulnerable to energy deprivation.

## 2 | MATERIALS AND METHODS

### 2.1 | Cell culture

Human MSC used in this study (Passages 5–7) were isolated from the bone marrow of healthy individuals ( $n = 5 \geq 56$ -years old, two females and three males, aged MSC;  $n = 5 \leq 20$ -years old, two females and three males, juvenile MSC), following standard

protocols published elsewhere (Angelova et al., 2018). Both MSC groups were characterized following the International Society for Cellular Therapy minimal definition criteria (Dominici et al., 2006; Horwitz et al., 2005), including plastic adherence, immunophenotype, and differentiation properties into mesodermal derivatives (data not shown), as described in previous studies (Barilani et al., 2016, 2015). Written informed consent was obtained from all the donors involved in the study. All experiments were performed according to the amended Declaration of Helsinki under the evaluation of the Ethical Committee of Fondazione IRCCS Ca' Granda Ospedale Maggiore Policlinico n° 1982, January 14, 2020. The culture medium consisted of  $\alpha$ -minimal essential medium-GlutaMAX (Thermo Fisher Scientific) supplemented with 10% fetal bovine serum (FBS; Thermo Fisher Scientific) and medium changes were performed twice a week. Cell cultures were maintained at 37°C in a humidified atmosphere containing 5% CO<sub>2</sub>. At 80% confluence, the cells were harvested using 25% TrypLE Select 1X (Thermo Fisher Scientific) and were washed with phosphate-buffered saline (Thermo Fisher Scientific) and cultured at a concentration of  $4 \times 10^3$  cells/cm<sup>2</sup>.

### 2.2 | Live-cell imaging

#### 2.2.1 | Mitochondrial membrane potential ( $\Delta\Psi_m$ ) measurements

For measurements of  $\Delta\Psi_m$ , cells plated on 25-mm glass coverslips were loaded for 30 min at room temperature (RT) with 25 nM tetramethylrhodamine methyl ester (TMRM; Invitrogen) in a HEPES-buffered saline solution (HBSS) composed of 156 mM NaCl, 3 mM KCl, 2 mM MgSO<sub>4</sub>, 1.25 mM KH<sub>2</sub>PO<sub>4</sub>, 2 mM CaCl<sub>2</sub>, 10 mM glucose, and 10 mM HEPES; pH adjusted to 7.35 with NaOH. The dye remained present in the media at the time of recording. Confocal images were obtained using a Zeiss 710 VIS CLSM equipped with a META detection system and a  $\times 40$  oil immersion objective. TMRM was excited using the 560 nm laser line and fluorescence was measured above 580 nm (M. H. R. Ludtmann et al., 2018). For basal  $\Delta\Psi_m$  measurements, Z-stack images were obtained by confocal microscopy and analyzed using Zeiss software. For analysis of response to mitochondrial toxins, images were recorded continuously from a single focal plane. TMRM is used in the redistribution mode to assess  $\Delta\Psi_m$ , and, therefore, a reduction in TMRM fluorescence represents mitochondrial depolarization.

#### 2.2.2 | Measurement of NADH/flavin adenine dinucleotide redox index and pool

NADH autofluorescence was measured using an epifluorescence inverted microscope equipped with a  $\times 20$  fluorite objective. Excitation light at a wavelength of 350 nm was provided by a Xenon arc lamp, the beam passing through a monochromator (Cairn Research).

Emitted fluorescence light was reflected through a 455 nm long-pass filter to a cooled charge-coupled device (CCD) camera (Retiga; QImaging) and digitized to 12-bit resolution. Imaging data were collected and analyzed using software from Andor. Flavin adenine dinucleotide (FAD) autofluorescence was monitored using a Zeiss 710 VIS CLSM equipped with a META detection system and a  $\times 40$  oil immersion objective. Excitation was using the 454 nm Argon laser line and fluorescence was measured from 505 to 550 nm. Illumination intensity was kept to a minimum (at 0.1%–0.2% of laser output) to avoid phototoxicity and the pinhole set to give an optical slice of  $\sim 2 \mu\text{m}$ . FAD and NADH redox indexes and mitochondrial pools were estimated according to previously described (Al-Menhali et al., 2020).

### 2.2.3 | Mag-Fura2 measurements

To assess the ATP levels, which correlate with the release of  $\text{Mg}^{2+}$  upon degradation of the ATP-Mg complex,  $[\text{Mg}^{2+}]_c$  was imaged using Mag-Fura2 AM according to (M. H. Ludtmann et al., 2016). Fluorescence images were acquired at a 30 s interval on an epifluorescence inverted microscope equipped with a  $\times 20$  fluorite objective (upon excitation at 340 and 380 nm). The emitted light was reflected through a 515 nm long-pass filter to a cooled CCD camera (Retiga; QImaging) and digitized to 12-bit resolution (Cairn Research). Andor iQ3 software was used to collect and analyze data.

### 2.2.4 | mtDNA content assessment

mtDNA content in live cells was assessed using Quant-iT PicoGreen dsDNA probe (Molecular Probes Inc.) at  $3 \mu\text{M}$  directly into the cell culture medium. The cells were then incubated for 30 min, under standard culture conditions ( $37^\circ\text{C}$ , 5%  $\text{CO}_2$ ) according to (Angelova et al., 2018). The cells were then rinsed 3X in prewarmed HBSS and visualized using a Zeiss 710 VIS CLSM equipped with a META detection system under  $\times 40$  magnification. Excitation was using the 488 nm Argon laser line and fluorescence was measured from 510 to 550 nm.

### 2.2.5 | Mitochondrial colocalization with lysosomes

For visualization of the mitolysosome formation (late phase of mitophagy), we have used the colocalization of mitochondrial and lysosomal signals. Cells were loaded with 200 nM MitoTracker Green FM and 50 nM LysoTracker Red in HBSS for 30 min before experiments as described previously (Berezhnov et al., 2016). Confocal images were obtained using a Zeiss 710 confocal microscope equipped with a  $\times 40$  oil immersion objective. The 488 nm Argon laser line was used to excite MitoTracker Green fluorescence which was measured between 505 and 530 nm. Illumination intensity was kept to a minimum (about 1% of laser output) to avoid phototoxicity and

the pinhole set to give an optical slice of  $\sim 2 \mu\text{m}$ . For LysoTracker Red, the 543 nm Ne/He laser line was used with measurements above 650 nm. All data presented were obtained from at least five coverslips and 2–3 different cell preparations.

### 2.2.6 | Mitochondrial reactive oxygen species measurements

For measurement of mitochondrial reactive oxygen species (ROS) production, cells were preincubated with MitoTracker Red CM-H<sub>2</sub>XROS for 10 min at RT. MitoTracker Red CM-H<sub>2</sub>XROS measurements were produced using 560 nm excitation and emission above 580 nm (Angelova et al., 2021).

### 2.2.7 | Glutathione level assessment

MSC was incubated with 50  $\mu\text{M}$  monochlorobimane (MCB) (Molecular Probes, Invitrogen) for 40 min in HEPES-buffered salt solution before imaging (Arber et al., 2017). Cells were then washed with HEPES-buffered salt solution and images of the fluorescence of the MCB-glutathione (GSH) were acquired using a Zeiss 710 CLSM with excitation at 405 nm and emission at 435–485 nm.

### 2.2.8 | $\beta$ -galactosidase activity

$\beta$ -galactosidase staining was performed using the Senescence Cells Histochemical Staining Kit (CS0030; Sigma-Aldrich) as previously described (Barilani, Palorini, et al., 2019). Images of stained cells were acquired with a Nikon Eclipse TS100 microscope (Nikon). A total of 10 fields were screened, acquiring images from  $n = 2$  technical replicates (two separate wells of a six-well plate), to analyse for positive staining at least 50 cells for each MSC population ( $n = 5$  aged MSC vs.  $n = 5$  juvenile MSC).

### 2.2.9 | Quantitative polymerase chain reaction

Gene expression ( $n = 5$  aged MSC vs.  $n = 5$  juvenile MSC, by two independent experiments), telomere length, and mtDNA copy number (mtDNA<sub>cn</sub>;  $n = 11$  aged MSC vs.  $n = 6$  juvenile MSC, by two independent experiments) studies were performed by quantitative polymerase chain reaction (qPCR) as elsewhere described (Barilani et al., 2016; Barilani, Peli, et al., 2019). RNA was extracted by standard TRIzol protocol (Thermo Fisher Scientific), following manufacturer's instructions. DNA extracted with QIAamp DNA Blood Mini Kit (51104; Qiagen), following manufacturer's instructions. All amplification reactions were performed in  $n = 3$  replicates in 96-well plates on a CFX96 machine (Bio-Rad). The data analysis was carried out using CFX Manager software (Bio-Rad).

### 2.2.10 | Total ATP quantification

Total ATP in MSC ( $n = 7$  aged MSC vs.  $n = 7$  juvenile MSC, by two independent experiments) was quantified by the ATP Bioluminescence Assay Kit HS II (11699709001; Roche). All steps were performed on ice and all reagents and ATP standard curve were prepared as indicated by the manufacturer's instructions. Cells were diluted to 200,000 cells/ml in dilution buffer at pH in the range 7.6–8.0. Next, 50  $\mu$ l of cell dilution and ATP standards were aliquoted in  $n = 3$  replicates in 96-well white plates with flat wells. Chemiluminescent signal was generated by a 5-min incubation with 50  $\mu$ l of cell lysis reagent and subsequent addition of 100  $\mu$ l of luciferase reagent at RT. The signal was measured on a plate reader (Infinite 200 PRO; TECAN) equipped with Te-Injec reagent injectors (TECAN), using Magellan software v7.0 (TECAN) for automated protocol set up and implementation.

### 2.2.11 | Glucose consumption and lactate production

Glucose and lactate levels were measured with StatStrip meters (Nova Biomedicals). Cells were seeded at 30,000 cells/cm<sup>2</sup>. The day after, the medium was changed with basal medium without FBS and collected 24 h later for glucose and lactate measurements. The amounts of consumed glucose and produced lactate were calculated based on initial concentrations ( $n = 5$  aged MSC vs.  $n = 5$  juvenile MSC).

## 2.3 | Statistical analysis

Data and statistical analysis were performed using Prism 6 (GraphPad Software) and OriginPro, Version 2019 (OriginLab Corporation). Details of statistical analyses are specified in the figure legends. A  $p < 0.05$  was considered statistically significant.

## 3 | RESULTS

### 3.1 | MSCs from older individuals recapitulate senescent traits

To validate in vitro cultured MSC as a model for in vivo aging, specific hallmarks of aging were investigated. First,  $\beta$ -galactosidase activity was addressed by a colorimetric assay as the main phenotypic feature of senescent cells. MSC from older individuals (aged MSC,  $n = 5$ ; an average of  $65.2 \pm 5.4$  years old) showed a significantly higher percentage of  $\beta$ -galactosidase-positive cells compared to MSC from younger individuals (juvenile MSC,  $n = 5$ ; an average of  $16.8 \pm 4.4$  years old) (Figure 1a,b). The latter presented a value consistent with MSC isolated from fetal tissue (Barilani, Palorini et al., 2019). Second,

qPCR analyses were performed to corroborate the  $\beta$ -galactosidase result. The gene expression of p21, a crucial protein involved in cell cycle control, was found to be significantly higher in aged MSC than in juvenile MSC (Figure 1c). Furthermore, telomere's length was determined, and a significant decrease was detected in aged MSC compared to juvenile MSC (Figure 1d). This is of particular interest, as telomere erosion is directly involved in the aging process. Finally, the gene expression of anti-inflammatory and proinflammatory cytokines was addressed. Consistent with a senescent phenotype, aged MSC showed increased levels of interleukin (IL)-6 and tumor necrosis factor- $\alpha$  messenger RNA, two major inflammatory cytokines, together with a decreased level of IL-10, the most known anti-inflammatory cytokine, compared to juvenile MSC (Figure 1e).

### 3.2 | Basal mitochondrial membrane potential declines with age

Mitochondrial membrane potential ( $\Delta\Psi_m$ ) is the major indicator of any changes in mitochondrial metabolism and related processes in this organelle. We used TMRM to assess  $\Delta\Psi_m$  in aged and juvenile MSC. Mitochondrial membrane potential in aged MSC was significantly lower compared to juvenile MSC (58.6%,  $n = 5$ , 66.9%,  $n = 5$ ; first young control was taken as 100%,  $n = 5$ ; Figure 2a,b).

Mitochondrial membrane potential is maintained mostly by the function of the electron transport chain (ETC). However, in case of pathology or lack of oxygen, it can be compensated by the  $F_0-F_1$ -ATPase, which consumes ATP to pump protons to keep  $\Delta\Psi_m$  in an optimal range (Abramov & Angelova, 2019b). Oligomycin can block both  $F_0-F_1$ -ATPase and synthase functions. We take advantage of its effects to assess whether partial depolarization of mitochondria, the result of the reversal of ATP-synthase, takes place with aging. Application of 2  $\mu$ g/ml oligomycin to juvenile MSC induced a small increase or no changes in  $\Delta\Psi_m$  (Figure 2c,d) that suggested that membrane potential was maintained by ETC. The use of 5  $\mu$ M inhibitor of complex I rotenone surprisingly had only a moderate effect on these cells and reduced  $\Delta\Psi_m$  only by 26% ( $N = 6$ ) and 12% ( $N = 6$ ; Figure 2c,d) that suggests a relatively low activity of complex I in juvenile MSC. The addition of 1  $\mu$ M of the protonophore carbonyl cyanide p-trifluoromethoxy)phenylhydrazone (FCCP) led to a complete depolarization of the mitochondrial membrane, which (after the addition of oligomycin and rotenone) could correspond to the implication of complex II in the maintenance of  $\Delta\Psi_m$  and in case of juvenile MSC it was  $72.9\% \pm 3.8\%$  and  $89.3\% \pm 5.7\%$  (Figure 2c,d). Aged MSC generated a small decrease of  $\Delta\Psi_m$  in response to oligomycin (12% and 11%,  $N = 7$ ) that suggested partial compensation of the signal by  $F_0-F_1$ -ATPase, working in reverse mode. The effect of 5  $\mu$ M rotenone was also higher in aged MSC compared to juvenile MSC (45% and 44%; Figure 2e,f). The final decrease by FCCP was  $38.2\% \pm 3.2\%$  and  $45.5\% \pm 2.8\%$  (Figure 2e,f). These data suggested a shift not only in the range of  $\Delta\Psi_m$  in aged MSC but also changes in the mechanism of its maintenance with aging.

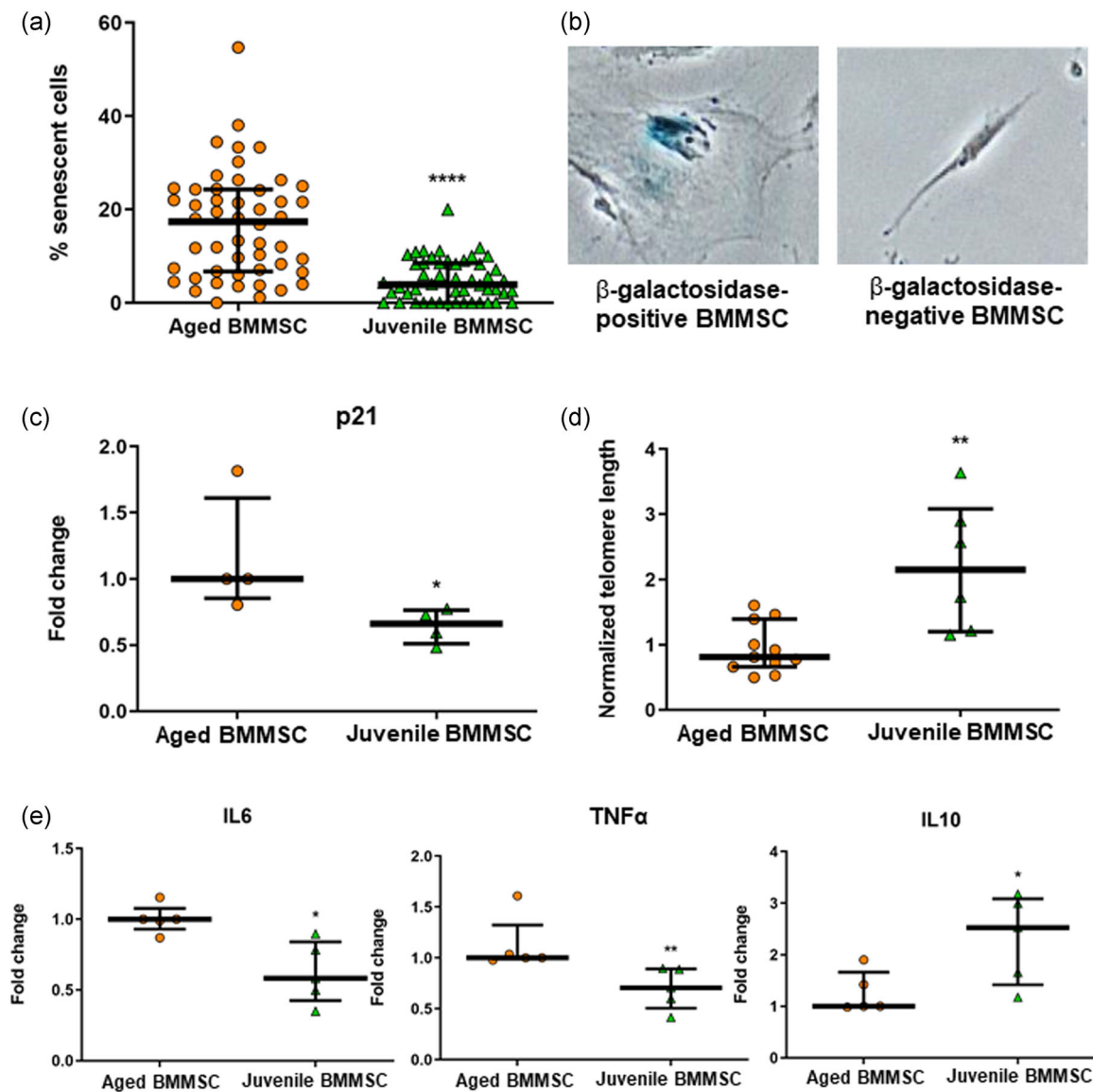


**FIGURE 1** Senescence status of aged MSC compared with juvenile MSC. (a) Scatter dot plot shows the percentage of senescent cells (%) in aged and juvenile MSC. Median and interquartile ranges are represented. (b) Representative bright-field images of senescent ( $\beta$ -galactosidase-positive MSC) and nonsenescent ( $\beta$ -galactosidase-negative MSC) cells. (c) Scatter dot plots show fold change of p21 gene expression normalized to aged MSC. Median and interquartile ranges are represented. (d) Scatter dot plots show telomere length normalized to aged MSC. Median and interquartile ranges are represented. (e) Scatter dot plots show fold change of IL-6, TNF- $\alpha$ , and IL-10 gene expression normalized to aged MSC. Median and interquartile ranges are represented. Statistical analyses were by two-tailed nonparametric Mann-Whitney test for (a, c, and e), and by Kolmogorov-Smirnov normality test followed by two-tailed parametric Student's *t*-test for (d); \**p* < 0.05, \*\**p* < 0.01, \*\*\*\**p* < 0.0001, *n* = 5, for each experimental group. BMMSC, bone marrow mesenchymal stem cell; IL-6, interleukin-6; MSC, mesenchymal stem cell; TNF- $\alpha$ , tumor necrosis factor- $\alpha$

### 3.3 | NADH and FAD-dependent respiration changes with the age of the MSC donor

The level of substrates for Complex I and Complex II, NADH and FADH, can be measured as the autofluorescence of the latter. To separate the autofluorescence of mitochondrial NADH and FAD from NADPH and cytosolic NADH and FAD, we used the mitochondrial uncoupler FCCP and the inhibitor of respiration NaCN. FCCP maximizes respiration and minimizes the substrates

NADH (taken as 0%) and FADH, while FAD, in contrast, increases (taken as 100%). NaCN blocks respiration and substrate consumption which results in an increase in NADH to maximal level (taken as 100%) but leads to the decrease of FAD (due to increased FADH) to a minimum level (taken as 0%). Using these data, we estimated the mitochondrial pool of NADH and FAD/FADH and also the respiratory activity (redox state) as a balance between production and consumption of these substrates (in normalized Figure 3a,b correspond to the basal values). We have

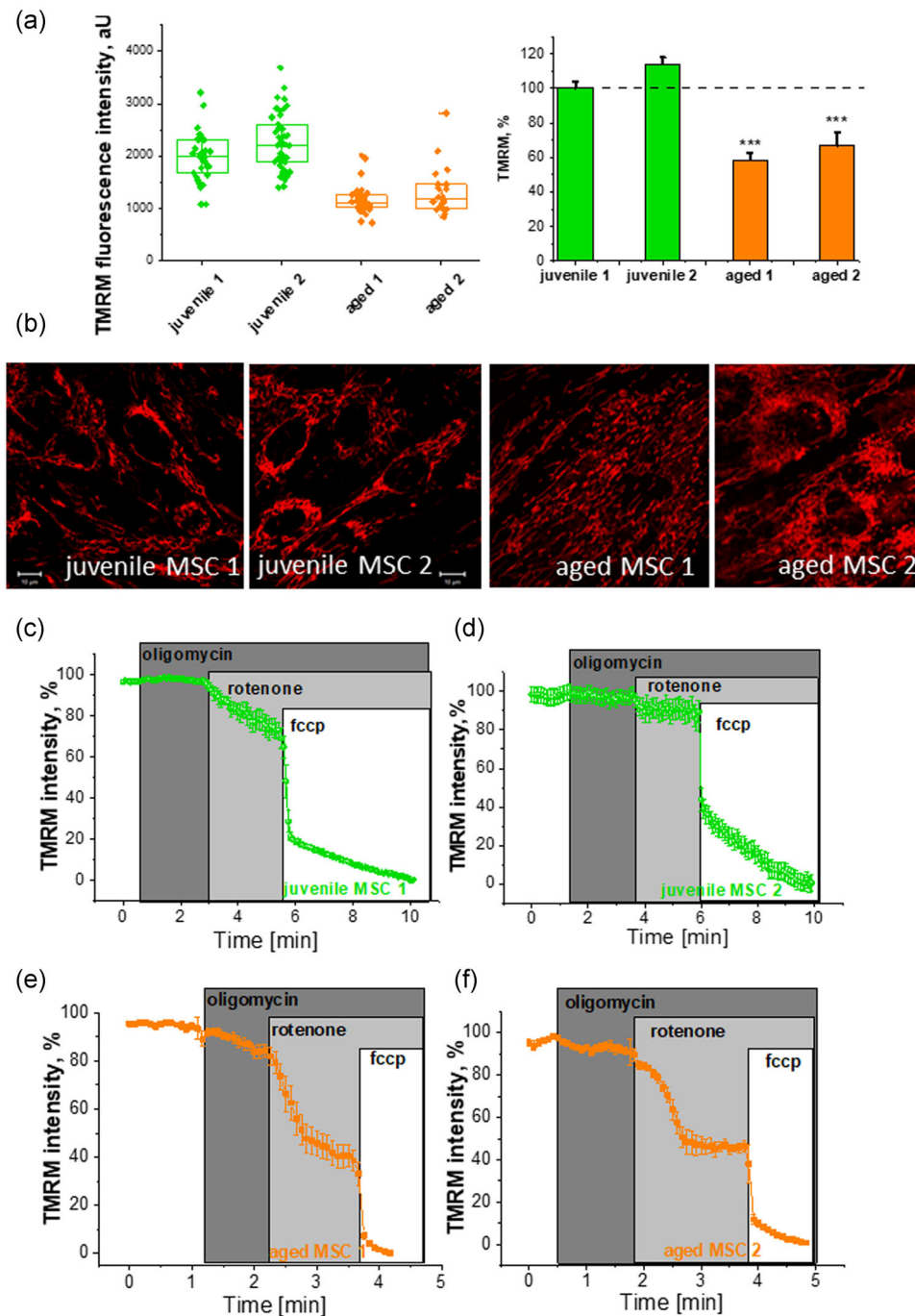


**FIGURE 2** Mitochondrial membrane potential is decreased in aged MSC. (a) Changes in  $\Delta\Psi_m$  (TMRM fluorescence) between young and aged MSC. (b) Representative images of TMRM fluorescence of young and aged MSC. Changes in the maintenance of  $\Delta\Psi_m$  in aged (e, f) compared to younger (c, d) MSC. 2  $\mu\text{g}/\text{ml}$  oligomycin, 1  $\mu\text{M}$  rotenone, and 1  $\mu\text{M}$  FCCP were applied to cells during experiments. Statistical analysis was done by two-tailed parametric Student's *t*-test, preceded by Kolmogorov–Smirnov normality test,  $***p > 0.0001$ . FCCP, carbonyl cyanide *p*-trifluoromethoxyphenylhydrazone; MSC, mesenchymal stem cell; TMRM, tetramethylrhodamine methyl ester

found that NADH redox index was reduced in aged MSC (from  $74 \pm 5$ ,  $N = 7$  to  $47 \pm 5.1$ ,  $N = 7$ ; Figure 3a–c). Mitochondrial NADH pool in aged MSC was significantly decreased (from  $171.2 \pm 28.2$ ,  $N = 7$  to  $60.4 \pm 10.1$ ,  $N = 7$ , Figure 3a,c). Taken together, higher respiratory activity in aged MSC leads to a reduction of the mitochondrial NADH pool that is in agreement with responses to

rotenone addition in the  $\Delta\Psi_m$  measurement. Importantly, the FAD redox index was significantly higher in aged MSC than in juvenile MSC (Figure 3d,e) confirming higher respiratory activity in these cells. However, we have not found any highly significant differences in mitochondrial FAD pool between the pooled aged and young MSC data (Figure 3d,f).

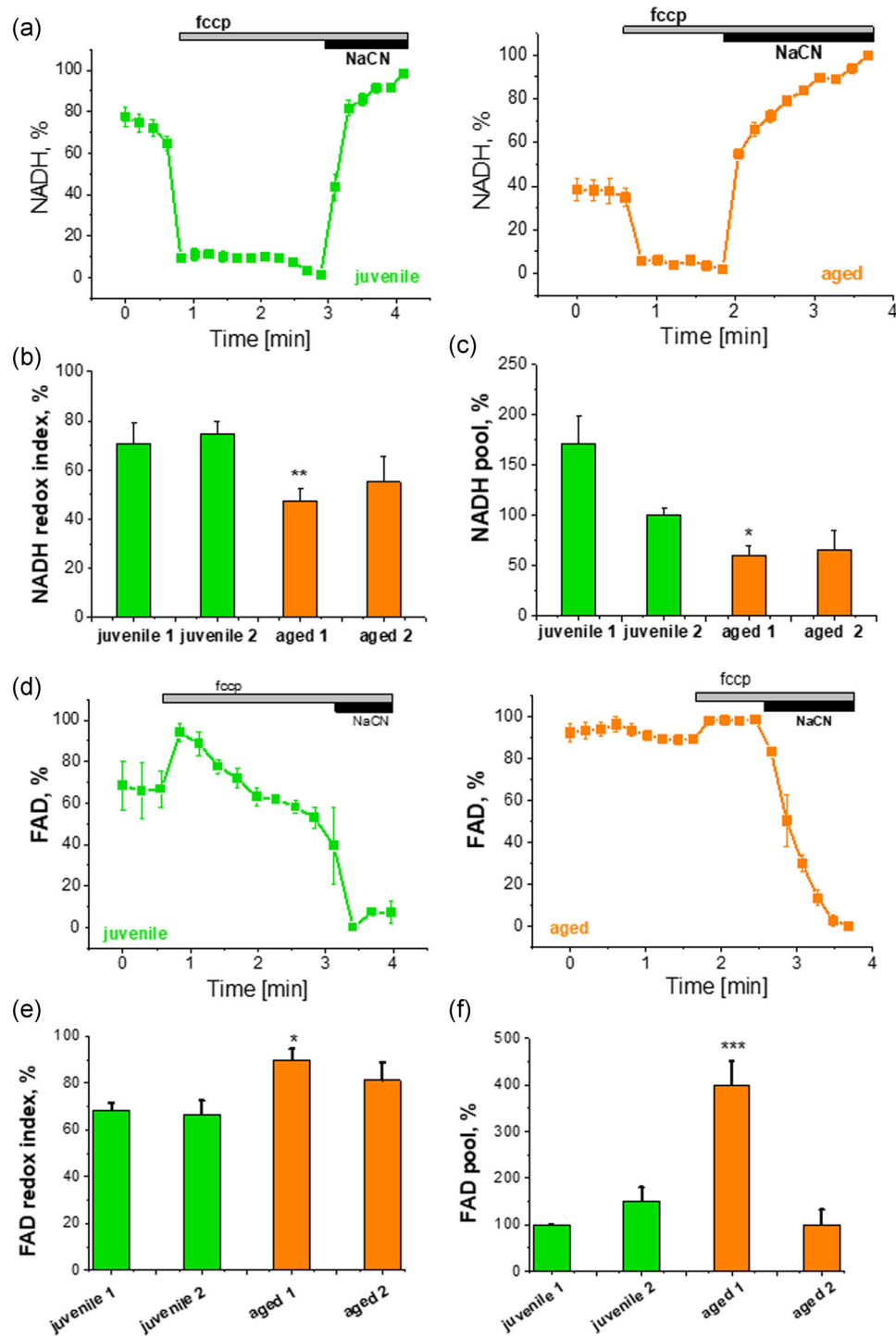


**FIGURE 3** Age-related activation of NADH and FADH dependent respiration in MSC. (a) Representative traces of NADH autofluorescence in young and aged MSC in response to 1  $\mu$ M FCCP and 1 mM NaCN. Quantification of the NADH redox index (b) and mitochondrial NADH pool (c) calculated for young and aged MSC. (d) Representative traces of FAD autofluorescence in young and aged MSC in response to 1  $\mu$ M FCCP and 1 mM NaCN. Quantification of the FAD redox index (e) and mitochondrial FAD pool (f) calculated in young and aged MSC. Statistical analysis was done by two-tailed parametric Student's *t*-test, preceded by Kolmogorov-Smirnov normality test, \* $p < 0.05$ , \*\* $p < 0.01$ , \*\*\* $p > 0.0001$ . FAD, flavin adenine dinucleotide; FCCP, carbonyl cyanide *p*-trifluoromethoxy)phenylhydrazone; MSC, mesenchymal stem cell

### 3.4 | Aged MSC have a lower glucose uptake and glycolytic activity

The lower level of mitochondrial NADH pool could be explained by lower glucose uptake and glycolytic activity, which results in lower pyruvate production, or alteration of the Krebs cycle. To address these aspects, both glucose consumption and lactate production in the culture medium were measured. Aged MSC revealed significantly lower glucose consumption (Figure 4a) and lactate production (Figure 4b), consistent with the lower level of

mitochondrial NADH pool. To corroborate this hypothesis, total ATP content was measured. As shown in Figure 4c, aged MSC produced significantly higher amounts of ATP despite lower glucose consumption, confirming preference for oxidative phosphorylation (OXPHOS). ATP balance in the cells is maintained not only by the production of ATP in glycolysis and OXPHOS, but also by the rate of ATP consumption (Abramov & Angelova, 2019a; Abramov & Duchen, 2010). To measure ATP consumption, we used Mag Fura-2. Magnesium is released from Mg-ATP complexes upon hydrolysis of ATP (Leyskens et al., 1996), and,

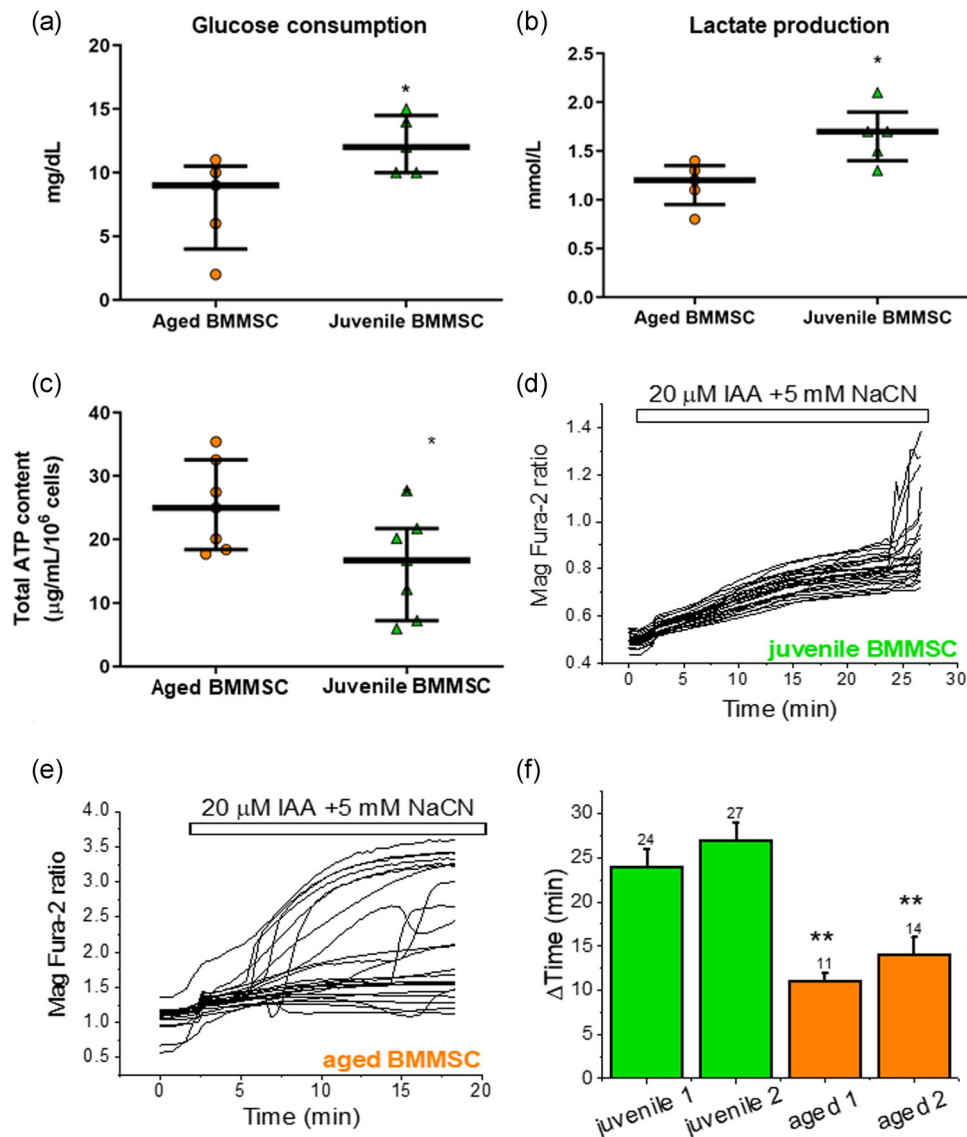


**FIGURE 4** ATP production and ATP consumption in aged and young MSC. Scatter dot plots show glucose consumption (a) and lactate production (b) during 24 h for aged and juvenile MSC. Median and interquartile ranges are represented. (c) Scatter dot plots show total ATP quantification normalized to 1 million cells for aged and juvenile MSC. Median and interquartile ranges are represented. Statistical analyses were done by Kolmogorov–Smirnov normality test followed by two-tailed parametric Student's *t*-test; \**p* < 0.05, *n* = 5 for (a, b), *n* = 7 for (c), each experimental group. Representative traces of Mag-Fura-2 ratio in young (d) and aged (e) MSC in response to 20 µM IAA and 5 mM NaCN. Each trace represents a measurement from a single cell. (f) Quantification of the time to collapse after inhibition of ATP production in young and aged MSC. Statistical analysis was done by two-tailed parametric Student's *t*-test, preceded by Kolmogorov–Smirnov normality test, \**p* < 0.05, \*\**p* < 0.01. BMMSC, bone marrow mesenchymal stem cell; MSC, mesenchymal stem cell; IAA, iodoacetic acid

therefore, a measurement of cellular free magnesium, can be used as an indication of ATP consumption rates. Application of inhibitors of glycolysis (20  $\mu$ M iodoacetic acid [IAA]) and of the OXPHOS (2  $\mu$ g/ml oligomycin) blocks the ATP production, resulting in an increase in the MagFura-2 fluorescence. MagFura-2 is also used as a low-affinity  $\text{Ca}^{2+}$  indicator that could also help to indicate cell lysis due to energy collapse and inability to maintain cellular calcium homeostasis. However, previously we found that inhibition of mitochondrial respiration with NaCN induced even faster collapse of the cells because of additional consumption of ATP in  $\text{F}_0\text{-F}_1\text{-ATPase}$  (M. H. Ludtmann et al., 2016). In our experiments, application of 20  $\mu$ M IAA and 5 mM NaCN led to energy collapse in young ( $n = 314$  cells; Figure 4d) and aged MSC ( $n = 290$  cells; Figure 4e). Despite the higher ATP content in aged cells (Figure 4c), time to energy collapse in young cells was significantly longer, compared to the aged MSC collapse time (Figure 4d–f). This strongly suggests the lower rate of consumption of ATP in the juvenile MSC.

### 3.5 | Higher mtDNA content in aged MSC

To explain higher OXPHOS activity in aged MSC, the level of mtDNA was estimated using the fluorescent probe PicoGreen. In our experiments, the level of nuclear PicoGreen fluorescence was similar between all MSC populations (Figure 5a). However, PicoGreen-DNA fluorescence from the mitochondrial area was significantly higher in aged MSC (Figure 5a,b). To confirm this result, mtDNAcn was determined also by qPCR. As shown in Figure 5c, aged MSC resulted in significantly higher mtDNAcn.

### 3.6 | Mitochondrial mass in aged MSC

Taken together, these data hinted at a higher level of mitochondrial biogenesis in aged MSC, which should lead to increasing in mitochondrial mass. To identify it, we calculated the optical density of mitochondrial (TMRM) fluorescence per area of the cell. We have found that the mitochondrial mass was lower in aged MSC than in juvenile MSC (Figure 5d). This result was consistent with the higher gene expression of mitochondrial biogenesis driver transcription factor A, mitochondrial (Figure 5e).

Higher mtDNAcn accompanied by a lower content of mitochondria might be explained by the faster rate of mitochondrial degradation (mitophagy). To test this hypothesis, we measured the level of mitophagy as the colocalization of mitochondrial fluorescence (MitoTracker Green) with lysosome fluorescence (LysoTracker Red). Younger MSC had a threefold lower percentage of mitochondria colocalization with lysosomes than aged MSC (Figure 5f,g). Thus, the increased rate of mitophagic degradation of mitochondria in aged MSC decreased mitochondrial mass despite the significantly higher levels of mtDNA.

### 3.7 | Aged MSC induce a higher rate of ROS in mitochondria

Abnormal mitochondrial metabolism can lead to excessive ROS production and oxidative stress (Angelova and Abramov, 2016). In our experiments, aged MSC had a higher rate of MitoTracker Red CM-H(2)XROS fluorescence ( $424\% \pm 19\%$ ,  $N = 6$ ; and  $309\% \pm 28\%$  of juvenile MSC; Figure 6a,c) that suggests an enhanced level of ROS production inside the mitochondrial matrix. Mitochondrial ROS could be used by cells in physiological signaling, but they could damage the cells in case of excessive production, that is, oxidative stress (Angelova, 2021). To identify whether the high level of ROS production in mitochondria of aged MSC can induce oxidative stress we measured the level of the major endogenous antioxidant GSH. We have found that both aged MSC lines had a higher level of GSH (Figure 6d,e). Consistent with this result, expression of genes involved in response to oxidative stress (NRF2, SOD1, and CAT) determined by qPCR was not upregulated in aged MSC compared with juvenile MSC (Figure 6f). Thus, despite the increased rate of ROS production in mitochondria of aged MSC, this did not produce oxidative stress in the cells.

## 4 | DISCUSSION

The issue of whether and to which extent aging influences MSC properties has been raising interest for many years (Schimke et al., 2015). This area of research has the aim to investigate the usefulness of bone marrow harvest from old donors in the context of an aging western population and to assess the therapeutic potential of its cellular derivatives. Recently, the role of metabolism and mitochondrial function in stem cell fate choices and behavior gained higher and higher attention, in particular, with regard to pathological conditions and aging (Barilani, Palorini, et al., 2019; Zhang et al., 2018).

In this scenario, we assessed the senescence status and studied the mitochondrial activity of MSC derived from young and old bone marrow donors to address chronological aging. Consistent with previous studies (Baxter et al., 2004; Beane et al., 2014; Block et al., 2017; Chen et al., 2014; Gnani et al., 2019; Guillot et al., 2007; Oda et al., 2010; Stenderup et al., 2003; Stolzing et al., 2008), our results indicated that aged MSC showed senescent traits compared with juvenile MSC, including  $\beta$ -galactosidase activity, p21 gene expression, telomeres erosion, and transcript levels of inflammatory cytokines, which are major components of the senescence-associated secretory phenotype.

Regarding mitochondrial activity, we observed that aged MSC possess lower  $\Delta\Psi_m$  and more fragmented morphology (see Figure 2b), with broad cytoplasmic localization, in line with other studies performed mainly on rodents (Geissler et al., 2012; Mantovani et al., 2012; Pietilä et al., 2012). Our study addressed more deeply the molecular mechanism of  $\Delta\Psi_m$  maintenance. Intriguingly, our data suggested a role for Complex I and the proton

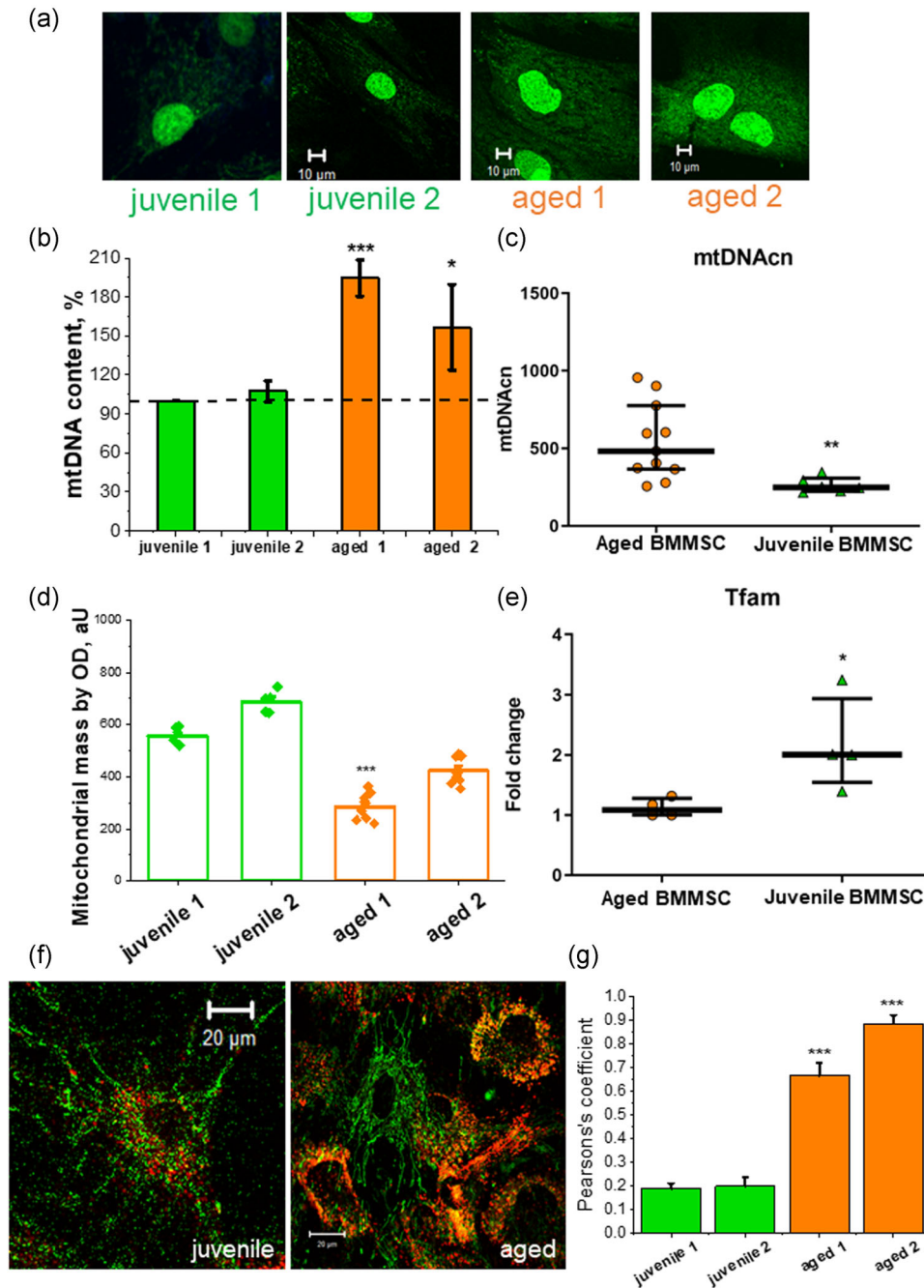


**FIGURE 5** Mitochondrial mass of aged MSC compared with juvenile MSC. (a) Representative images of mitochondrial DNA content in aged and juvenile MSC assessed with Quant-iT PicoGreen dsDNA probe. (b) Quantification bar chart of mitochondrial DNA (mtDNA) content in aged and juvenile MSC. (c) Scatter dot plots show absolute quantification of mitochondrial DNA copy numbers (mtDNAcn) for aged and juvenile MSC. Median and interquartile ranges are represented. (d) Quantification bar chart of the mitochondrial mass in aged and juvenile MSC. (e) Scatter dot plots show fold change of TFAM gene expression normalized to aged MSC. Median and interquartile ranges are represented. (f) Representative images of mitolysosomes formation in aged and juvenile MSC using colocalization of MitoTracker Green FM and LysoTracker Red DND-99. (g) A number of mitochondria fused with the lysosomes, a mitophagy rate measure, expressed via Pearson's correlation coefficient. Statistical analyses were by two-tailed nonparametric Mann-Whitney test for (c, e); \* $p < 0.05$ , \*\* $p < 0.01$ , \*\*\* $p > 0.0001$ ,  $n = 11$  (aged MSC) and  $n = 6$  (juvenile MSC) for (c),  $n = 5$  each experimental group for (e). BMMSC, bone marrow mesenchymal stem cell; MSC, mesenchymal stem cell; OD, optical density; TFAM, transcription factor A, mitochondrial

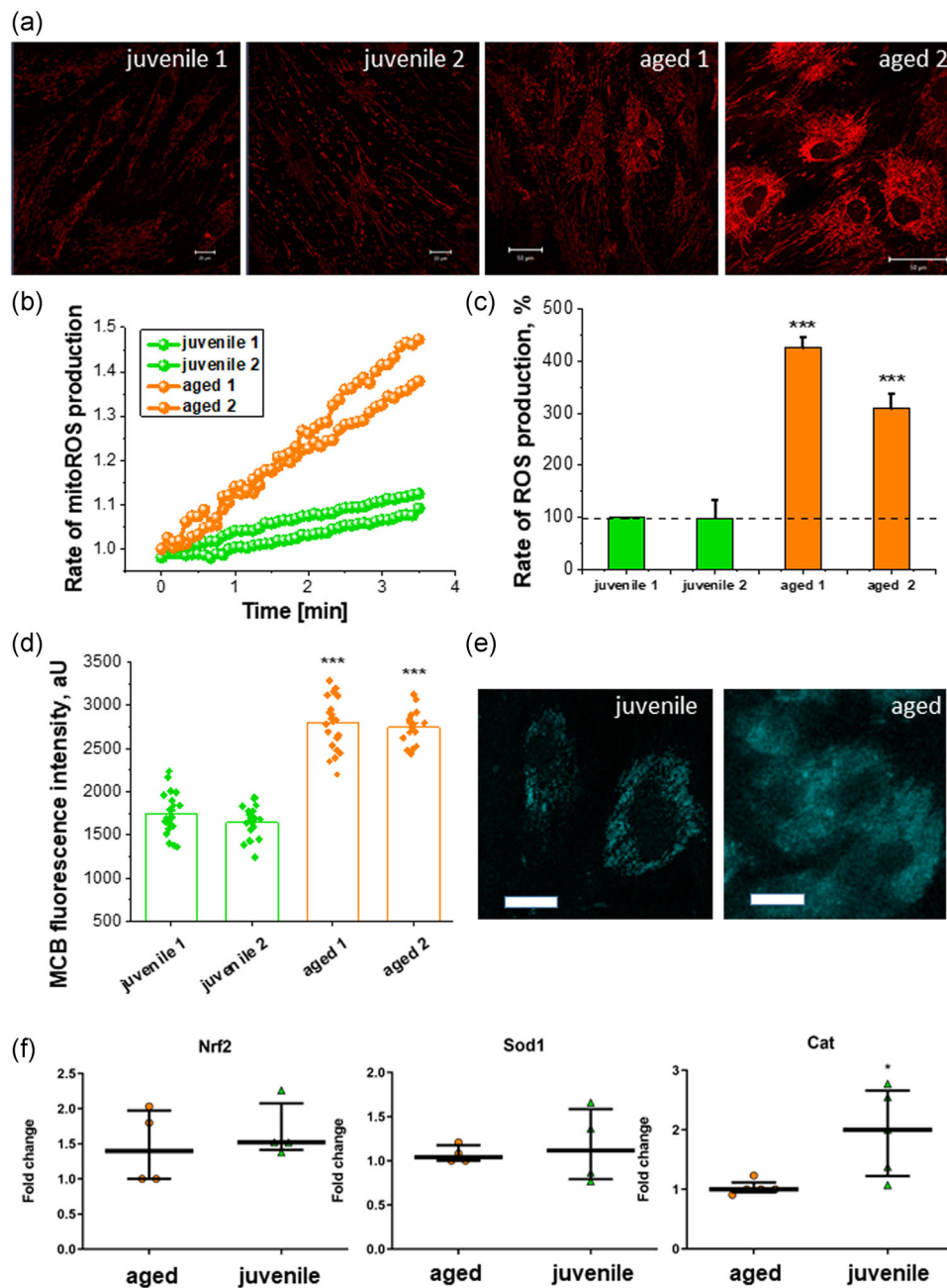


**FIGURE 6** The rate of ROS production and GSH level in aged MSC compared to juvenile MSC. (a) Representative images of basal mitochondrial ROS production in aged and juvenile MSC using MitoTracker Red CM-H(2)XROS. (b) Rate of ROS generation in aged and juvenile MSC expressed as change in MitoTracker Red CM-H(2)XROS intensity per minute. (c) Quantification bar chart of the data from (a and b). (d) Quantification bar charts showing glutathione levels in life aged and juvenile MSC. (e) Representative images of GSH levels using monochlorobimane. (f) Scatter dot plots show fold change of NRF2, SOD1, and CAT gene expression normalized to aged MSC. Median and interquartile ranges are represented. Statistical analyses were by two-tailed nonparametric Mann-Whitney test for (f); \* $p < 0.05$ , \*\*\* $p > 0.0001$ ,  $n = 5$  for each experimental group for (f). GSH, glutathione; MCB, monochlorobimane; MSC, mesenchymal stem cell; ROS, reactive oxygen species

pump in  $F_0-F_1$ -ATPase in the regulation of  $\Delta\Psi_m$  in aged MSC. In support of the major involvement of Complex I in the maintenance of aged MSC  $\Delta\Psi_m$ , we showed a lower NADH redox index and NADH pool. This could be due also to reduced expression of NAMPT and consequent depletion of  $NAD^+$  reserves following chronological aging, as shown by others in a rat model (C. Ma et al., 2017). Our

results showed higher total ATP content in aged MSC, accompanied by higher glucose consumption and decreased lactate production, hinting at a less glycolytic central metabolism.

Aged MSC showed increased mtDNAcn, but lower mitochondrial mass associated with enhanced mitophagy is in line with others (Pietilä et al., 2012). Sustained mtDNA synthesis was associated with

autophagy to provide sufficient nucleotides and prevent further increase of ROS levels in eukaryotic cells (Medeiros et al., 2018). Using rodent models, two studies showed reduced autophagy in aged bone marrow MSC and underlined the positive effect of this process in rescuing age-associated bone loss (Y. Ma et al., 2018; M. Yang et al., 2018). This might mean that human aged MSC is still capable of correctly inducing mitochondrial-specific autophagy to preserve their functionality in contrast to rodent aged MSC. This could also be explained by the fact that the rate of specific mitophagy could be different from the total rate of autophagy in the cells. Multiple mechanisms of mitophagy may be involved in the age-related processes in MSC including acidification of the cytosol with lactate (Komilova et al., 2021), Pink1/Parkin, or Fundc1-related mitophagy (Y. Wang et al., 2021; J. Wang et al., 2020).

To add crucial information for the interpretation of mitochondrial function or dysfunction, we also determined mitochondrial ROS production rate and antioxidant capacity of aged and juvenile MSC. Our results indicated the absence of oxidative stress despite the higher mitochondrial ROS levels in aged cells. Other studies tried to assess ROS levels and oxidative stress, again frequently relying on rodent bone marrow MSC, obtaining contrasting results (Block et al., 2017; Geissler et al., 2012; Pietilä et al., 2012; Shipounova et al., 2010; Stolzing et al., 2008; Ucer et al., 2017). It is worth noting that differences in human metabolism compared to that of rodents have been reported in the literature (Blais et al., 2017; Even et al., 2017; Martignoni et al., 2006).

Our hypothesis is that aged MSC has established a different but still functional bioenergetics program. This is in line with previous works focused only on MSC phenotypic and functional properties. In a context of consensus on lower bone marrow cellularity and frequency of MSC colonies upon isolation, impaired homeostasis in vivo was explained as a loss of mesenchymal progenitor numbers, rather than a reduction in their functionality. Consistently, human MSC from old and young bone marrow donors was shown by others to possess similar proangiogenic, immunomodulatory, and migration abilities (Andrzejewska et al., 2019; Lund et al., 2010). Likewise, others showed preservation of old rat bone marrow MSC functionality despite the presence of less organized mitochondria (Geissler et al., 2012; Mantovani et al., 2012).

All these data hint at a healthier mitochondrial activity of juvenile MSC, even though aged MSC altered bioenergetic program does not elicit cellular dysfunction. Furthermore, we showed that bone marrow MSC from donors of different ages can be used to model metabolic and mitochondrial activity changes depending on chronological aging and not on replicative senescence induced by repeated in vitro passaging of MSC isolated from the same donors. These results may have also a clinical impact on innovative therapeutic approaches involving MSC, such as mitochondrial transfer therapy (Islam et al., 2012). In this scenario, it would be pivotal to select the best source of mitochondria. Such a source should combine an abundance of mitochondrial mass with the presence of functional and dynamic mitochondria to allow for their mobilization following mechanisms that are still to be unveiled.

Our data strongly indicate the difference in bioenergetic status and the rate of metabolism in aged MSC. These results may be used in the development of stem cells replacement therapy and also for the development of a better strategy for healthy aging.

In conclusion, herein we addressed the mitochondrial activity of aged MSC compared with juvenile MSC and described a different, although functional, bioenergetics status. Notwithstanding, such phenotype may be sufficient to sustain stem cell self-renewal and fate choices.

## ACKNOWLEDGMENT

Plamena R. Angelova and Andrey Y. Abramov were supported by the Engineering and Physical Sciences Research Council (Grant No. EP/R024898/1).

## CONFLICT OF INTERESTS

The authors declare that there are no conflict of interests.

## AUTHOR CONTRIBUTIONS

**Mario Barilani:** Conceptualization, methodology, validation, formal analysis, investigation, data curation, visualization, and writing – original draft preparation, review and editing, and project administration. **Christopher Lovejoy:** Validation, formal analysis, and investigation. **Roberta Piras:** Methodology and writing – original draft preparation. **Andrey Y. Abramov:** Conceptualization, resources, supervision, and writing – original draft preparation and review and editing. **Lorenza Lazzari:** Conceptualization, resources, supervision, and writing – review and editing. **Plamena R. Angelova:** Conceptualization, methodology, validation, formal analysis, investigation, data curation, visualization, and writing – original draft preparation, review and editing, and project administration.

## ORCID

Mario Barilani  <http://orcid.org/0000-0003-2225-897X>

Andrey Y. Abramov  <http://orcid.org/0000-0002-7646-7235>

Plamena R. Angelova  <https://orcid.org/0000-0003-4596-9117>

## REFERENCES

- Abramov, A. Y., & Angelova, P. R. (2019a). Cellular mechanisms of complex I-associated pathology. *Biochemical Society Transactions*, 47(6), 1963–1969. <https://doi.org/10.1042/BST20191042>
- Abramov, A. Y., & Angelova, P. R. (2019b). Mitochondrial dysfunction and energy deprivation in the mechanism of neurodegeneration. *Turkish Journal of Biochemistry*, 44(6), 723–729. <https://doi.org/10.1515/tjb-2019-0255>
- Abramov, A. Y., & Duchon, M. R. (2010). Impaired mitochondrial bioenergetics determines glutamate-induced delayed calcium deregulation in neurons. *Biochimica et Biophysica Acta*, 1800(3), 297–304. <https://doi.org/10.1016/j.bbagen.2009.08.002>
- Ahmad, T., Mukherjee, S., Pattnaik, B., Kumar, M., Singh, S., Kumar, M., Rehman, R., Tiwari, B. K., Jha, K. A., Barhanpurkar, A. P., Wani, M. R., Roy, S. S., Mabalirajan, U., Ghosh, B., & Agrawal, A. (2014). Miro1 regulates intercellular mitochondrial transport & enhances mesenchymal stem cell rescue efficacy. *EMBO Journal*, 33(9), 994–1010. <https://doi.org/10.1002/emboj.201386030>

- Al-Menhali, A. S., Banu, S., Angelova, P. R., Barcaru, A., Horvatovich, P., Abramov, A. Y., & Jaganjac, M. (2020). Lipid peroxidation is involved in calcium dependent upregulation of mitochondrial metabolism in skeletal muscle. *Biochimica et Biophysica Acta*, 1864(3), 129487. <https://doi.org/10.1016/j.bbagen.2019.129487>
- Andrzejewska, A., Catar, R., Schoon, J., Qazi, T. H., Sass, F. A., Jacobi, D., Blankenstein, A., Reinke, S., Krüger, D., Streitz, M., Schlickeiser, S., Richter, S., Souidi, N., Beez, C., Kamhieh-Milz, J., Krüger, U., Zemojtel, T., Jürchott, K., Strunk, D., Geissler, S. (2019). Multi-parameter analysis of biobanked human bone marrow stromal cells shows little influence for donor age and mild comorbidities on phenotypic and functional properties. *Frontiers in Immunology*, 10, 2474. <https://doi.org/10.3389/fimmu.2019.02474>
- Angelova, P. R. (2021). Sources and triggers of oxidative damage in neurodegeneration. *Free Radical Biology and Medicine*, 173, 52–63. <https://doi.org/10.1016/j.freeradbiomed.2021.07.003>
- Angelova, P. R., & Abramov, A. Y. (2016). Functional role of mitochondrial reactive oxygen species in physiology. *Free Radical Biology and Medicine*, 100, 81–85. <https://doi.org/10.1016/j.freeradbiomed.2016.06.005>
- Angelova, P. R., Barilani, M., Lovejoy, C., Dossena, M., Viganò, M., Seresini, A., Piga, D., Gandhi, S., Pezzoli, G., Abramov, A. Y., & Lazzari, L. (2018). Mitochondrial dysfunction in Parkinsonian mesenchymal stem cells impairs differentiation. *Redox Biology*, 14, 474–484. <https://doi.org/10.1016/j.redox.2017.10.016>
- Angelova, P. R., Dinkova-Kostova, A. T., & Abramov, A. Y. (2021). Assessment of ROS production in the mitochondria of live cells. *Methods in Molecular Biology*, 2202, 33–42. [https://doi.org/10.1007/978-1-0716-0896-8\\_2](https://doi.org/10.1007/978-1-0716-0896-8_2)
- Arber, C., Angelova, P. R., Wiethoff, S., Tsuchiya, Y., Mazzacupa, F., Preza, E., Bhatia, K. P., Mills, K., Gout, I., Abramov, A. Y., Hardy, J., Duce, J. A., Houlden, H., & Wray, S. (2017). iPSC-derived neuronal models of PANK2-associated neurodegeneration reveal mitochondrial dysfunction contributing to early disease. *PLoS One*, 12(9), e0184104. <https://doi.org/10.1371/journal.pone.0184104>
- Barilani, M., Lavazza, C., Boldrin, V., Ragni, E., Parazzi, V., Crosti, M., Montelatici, E., Giordano, R., & Lazzari, L. (2016). A chemically defined medium-based strategy to efficiently generate clinically relevant cord blood mesenchymal stromal colonies. *Cell Transplantation*, 25(8), 1501–1514. <https://doi.org/10.3727/096368916x690827>
- Barilani, M., Lavazza, C., Viganò, M., Montemurro, T., Boldrin, V., Parazzi, V., Montelatici, E., Crosti, M., Moro, M., Giordano, R., & Lazzari, L. (2015). Dissection of the cord blood stromal component reveals predictive parameters for culture outcome. *Stem Cells and Development*, 24(1), 104–114. <https://doi.org/10.1089/scd.2014.0160>
- Barilani, M., Palorini, R., Votta, G., Piras, R., Buono, G., Grassi, M., Bollati, V., Chiaradonna, F., & Lazzari, L. (2019). Central metabolism of functionally heterogeneous mesenchymal stromal cells. *Scientific Reports*, 9(1):15420. <https://doi.org/10.1038/s41598-019-51937-9>
- Barilani, M., Peli, V., Cherubini, A., Dossena, M., Dolo, V., & Lazzari, L. (2019). NG2 as an identity and quality marker of mesenchymal stem cell extracellular vesicles. *Cells*, 8(12):1524. <https://doi.org/10.3390/cells8121524>
- Baxter, M. A., Wynn, R. F., Jowitt, S. N., Wraith, J. E., Fairbairn, L. J., & Bellantuono, I. (2004). Study of telomere length reveals rapid aging of human marrow stromal cells following in vitro expansion. *Stem Cells*, 22(5), 675–682. <https://doi.org/10.1634/stemcells.22-5-675>
- Beane, O. S., Fonseca, V. C., Cooper, L. L., Koren, G., & Darling, E. M. (2014). Impact of aging on the regenerative properties of bone marrow-, muscle-, and adipose-derived mesenchymal stem/stromal cells. *PLoS One*, 9(12), e115963. <https://doi.org/10.1371/journal.pone.0115963>
- Berezhnov, A. V., Soutar, M. P., Fedotova, E. I., Frolova, M. S., Plun-Favreau, H., Zinchenko, V. P., & Abramov, A. Y. (2016). Intracellular pH modulates autophagy and mitophagy. *Journal of Biological Chemistry*, 291(16), 8701–8708. <https://doi.org/10.1074/jbc.M115.691774>
- Blais, E. M., Rawls, K. D., Dougherty, B. V., Li, Z. I., Kolling, G. L., Ye, P., Wallqvist, A., & Papin, J. A. (2017). Reconciled rat and human metabolic networks for comparative toxicogenomics and biomarker predictions. *Nature Communications*, 8, 14250. <https://doi.org/10.1038/ncomms14250>
- Block, T. J., Marinkovic, M., Tran, O. N., Gonzalez, A. O., Marshall, A., Dean, D. D., & Chen, X. D. (2017). Restoring the quantity and quality of elderly human mesenchymal stem cells for autologous cell-based therapies. *Stem Cell Research & Therapy*, 8(1), 239. <https://doi.org/10.1186/s13287-017-0688-x>
- Chen, H., Liu, X., Zhu, W., Chen, H., Hu, X., Jiang, Z., Xu, Y., Wang, L., Zhou, Y., Chen, P., Zhang, N., Hu, D., Zhang, L., Wang, Y., Xu, Q., Wu, R., Yu, H., & Wang, J. (2014). SIRT1 ameliorates age-related senescence of mesenchymal stem cells via modulating telomere shelterin. *Frontiers in Aging Neuroscience*, 6, 103. <https://doi.org/10.3389/fnagi.2014.00103>
- Cho, Y. M., Kim, J. H., Kim, M., Park, S. J., Koh, S. H., Ahn, H. S., Kang, G. H., Lee, J. B., Park, K. S., & Lee, H. K. (2012). Mesenchymal stem cells transfer mitochondria to the cells with virtually no mitochondrial function but not with pathogenic mtDNA mutations. *PLoS One*, 7(3), e32778. <https://doi.org/10.1371/journal.pone.0032778>
- Cylus, J., Figueras, J., & Normand, C. (2019). European observatory policy briefs. In A. Sagan, E. Richardson, J. North, & C. White (Eds.), *Will population ageing spell the end of the welfare state? A review of evidence and policy options*. European Observatory on Health Systems and Policies.
- Demirovic, D., Nizard, C., & Rattan, S. I. (2015). Basal level of autophagy is increased in aging human skin fibroblasts in vitro, but not in old skin. *PLoS One*, 10(5), e0126546. <https://doi.org/10.1371/journal.pone.0126546>
- Dominici, M., Le Blanc, K., Mueller, I., Slaper-Cortenbach, I., Marini, F., Krause, D., Deans, R., Keating, A., Prockop, D. J., & Horwitz, E. (2006). Minimal criteria for defining multipotent mesenchymal stromal cells. The International Society for Cellular Therapy position statement. *Cytotherapy*, 8(4), 315–317. <https://doi.org/10.1080/14653240600855905>
- Even, P. C., Virtue, S., Morton, N. M., Fromentin, G., & Semple, R. K. (2017). Editorial: Are rodent models fit for investigation of human obesity and related diseases? *Frontiers in Nutrition*, 4, 58. <https://doi.org/10.3389/fnut.2017.00058>
- Ganguly, P., El-Jawhari, J. J., Burska, A. N., Ponchel, F., Giannoudis, P. V., & Jones, E. A. (2019). The Analysis of in vivo aging in human bone marrow mesenchymal stromal cells using colony-forming unit-fibroblast assay and the CD45(low)CD271(+) phenotype. *Stem Cells International*, 2019, 5197983. <https://doi.org/10.1155/2019/5197983>
- Ganguly, P., El-Jawhari, J. J., Giannoudis, P. V., Burska, A. N., Ponchel, F., & Jones, E. A. (2017). Age-related changes in bone marrow mesenchymal stromal cells: A potential impact on osteoporosis and osteoarthritis development. *Cell Transplantation*, 26(9), 1520–1529. <https://doi.org/10.1177/0963689717721201>
- Geissler, S., Textor, M., Kühnisch, J., Könnig, D., Klein, O., Ode, A., Pfizner, T., Adjaye, J., Kasper, G., & Duda, G. N. (2012). Functional comparison of chronological and in vitro aging: Differential role of the cytoskeleton and mitochondria in mesenchymal stromal cells. *PLoS One*, 7(12), e52700. <https://doi.org/10.1371/journal.pone.0052700>
- Gnani, D., Crippa, S., Della Volpe, L., Rossella, V., Conti, A., Lettera, E., Ravis, S., Omerti, M., Frascini, G., Bernardo, M. E., & Di Micco, R.

- (2019). An early-senescence state in aged mesenchymal stromal cells contributes to hematopoietic stem and progenitor cell clonogenic impairment through the activation of a pro-inflammatory program. *Aging cell*, 18(3), e12933. <https://doi.org/10.1111/acer.12933>
- Gómez-Barrena, E., Padilla-Eguiluz, N., Rosset, P., Gebhard, F., Hernigou, P., Baldini, N., Rouard, H., Sensebé, L., Gonzalo-Daganzo, R. M., Giordano, R., García-Rey, E., Cordero-Ampuero, J., Rubio-Suárez, J. C., García-Simón, M. D., Stanovici, J., Ehrnthaller, C., Huber-Lang, M., Flouzatz-Lachaniette, C. H., Chevallier, N., ... Layrolle, P. (2020). Early efficacy evaluation of mesenchymal stromal cells (MSC) combined to biomaterials to treat long bone non-unions. *Injury*, 51, 63. <https://doi.org/10.1016/j.injury.2020.02.070>
- Gu, Y., Li, T., Ding, Y., Sun, L., Tu, T., Zhu, W., Hu, J., & Sun, X. (2016). Changes in mesenchymal stem cells following long-term culture in vitro. *Molecular Medicine Reports*, 13(6), 5207–5215. <https://doi.org/10.3892/mmr.2016.5169>
- Guillot, P. V., Gotherstrom, C., Chan, J., Kurata, H., & Fisk, N. M. (2007). Human first-trimester fetal MSC express pluripotency markers and grow faster and have longer telomeres than adult MSC. *Stem Cells*, 25(3), 646–654. <https://doi.org/10.1634/stemcells.2006-0208>
- Han, H., Hu, J., Yan, Q., Zhu, J., Zhu, Z., Chen, Y., Sun, J., & Zhang, R. (2016). Bone marrow-derived mesenchymal stem cells rescue injured H9c2 cells via transferring intact mitochondria through tunneling nanotubes in an in vitro simulated ischemia/reperfusion model. *Molecular Medicine Reports*, 13(2), 1517–1524. <https://doi.org/10.3892/mmr.2015.4726>
- Hoffman, C. M., Han, J., & Calvi, L. M. (2019). Impact of aging on bone, marrow and their interactions. *Bone*, 119, 1–7. <https://doi.org/10.1016/j.bone.2018.07.012>
- Horwitz, E. M., Le Blanc, K., Dominici, M., Mueller, I., Slaper-Cortenbach, I., Marini, F. C., Deans, R. J., Krause, D. S., Keating, A., & International Society for Cellular, T. (2005). Clarification of the nomenclature for MSC: The International Society for Cellular Therapy position statement. *Cytotherapy*, 7(5), 393–395. <https://doi.org/10.1080/14653240500319234>
- Hsu, Y. C., Wu, Y. T., Yu, T. H., & Wei, Y. H. (2016). Mitochondria in mesenchymal stem cell biology and cell therapy: From cellular differentiation to mitochondrial transfer. *Seminars in Cell and Developmental Biology*, 52, 119–131. <https://doi.org/10.1016/j.semcdb.2016.02.011>
- Islam, M. N., Das, S. R., Emin, M. T., Wei, M., Sun, L., Westphalen, K., Rowlands, D. J., Quadri, S. K., Bhattacharya, S., & Bhattacharya, J. (2012). Mitochondrial transfer from bone-marrow-derived stromal cells to pulmonary alveoli protects against acute lung injury. *Nature Medicine*, 18(5), 759–765. <https://doi.org/10.1038/nm.2736>
- Kennedy, B. K., Berger, S. L., Brunet, A., Campisi, J., Cuervo, A. M., Epel, E. S., Franceschi, C., Lithgow, G. J., Morimoto, R. I., Pessin, J. E., Rando, T. A., Richardson, A., Schadt, E. E., Wyss-Coray, T., & Sierra, F. (2014). Geroscience: Linking aging to chronic disease. *Cell*, 159(4), 709–713. <https://doi.org/10.1016/j.cell.2014.10.039>
- Komilova, N. R., Angelova, P. R., Berezchnov, A. V., Stelmashchuk, O. A., Mirkhodjaev, U. Z., Houlden, H., Gourine, A. V., Esteras, N., & Abramov, A. Y. (2021). Metabolically induced intracellular pH changes activate mitophagy, autophagy, and cell protection in familial forms of Parkinson's disease. *FEBS Journal*. Advance online publication. <https://doi.org/10.1111/febs.16198>
- Kretlow, J. D., Jin, Y. Q., Liu, W., Zhang, W. J., Hong, T. H., Zhou, G., Baggett, L. S., Mikos, A. G., & Cao, Y. (2008). Donor age and cell passage affects differentiation potential of murine bone marrow-derived stem cells. *BMC Cell Biology*, 9, 60. <https://doi.org/10.1186/1471-2121-9-60>
- Leysens, A., Nowicky, A. V., Patterson, L., Crompton, M., & Duchon, M. R. (1996). The relationship between mitochondrial state, ATP hydrolysis, [Mg<sup>2+</sup>]<sub>i</sub> and [Ca<sup>2+</sup>]<sub>i</sub> studied in isolated rat cardiomyocytes. *The Journal of Physiology*, 496, 111–128.
- Lopez-Otin, C., Blasco, M. A., Partridge, L., Serrano, M., & Kroemer, G. (2013). The hallmarks of aging. *Cell*, 153(6), 1194–1217. <https://doi.org/10.1016/j.cell.2013.05.039>
- Ludtmann, M. H. R., Angelova, P. R., Horrocks, M. H., Choi, M. L., Rodrigues, M., Baev, A. Y., Berezchnov, A. V., Yao, Z., Little, D., Banushi, B., Al-Menhali, A. S., Ranasinghe, R. T., Whiten, D. R., Yalom, R., Dolt, K. S., Devine, M. J., Gissen, P., Kunath, T., Jaganjac, M., ... Gandhi, S. (2018). Alpha-synuclein oligomers interact with ATP synthase and open the permeability transition pore in Parkinson's disease. *Nature Communications*, 9(1), 2293. <https://doi.org/10.1038/s41467-018-04422-2>
- Ludtmann, M. H., Angelova, P. R., Ninkina, N. N., Gandhi, S., Buchman, V. L., & Abramov, A. Y. (2016). Monomeric alpha-synuclein exerts a physiological role on brain ATP synthase. *Journal of Neuroscience*, 36(41), 10510–10521. <https://doi.org/10.1523/JNEUROSCI.1659-16.2016>
- Lund, T. C., Kobs, A., Blazar, B. R., & Tolar, J. (2010). Mesenchymal stromal cells from donors varying widely in age are of equal cellular fitness after in vitro expansion under hypoxic conditions. *Cytotherapy*, 12(8), 971–981. <https://doi.org/10.3109/14653249.2010.509394>
- Ma, C., Pi, C., Yang, Y., Lin, L., Shi, Y., Li, Y., Li, Y., & He, X. (2017). Namp1 expression decreases age-related senescence in rat bone marrow mesenchymal stem cells by targeting Sirt1. *PLoS One*, 12(1), e0170930. <https://doi.org/10.1371/journal.pone.0170930>
- Ma, Y., Qi, M., An, Y., Zhang, L., Yang, R., Doro, D. H., Liu, W., & Jin, Y. (2018). Autophagy controls mesenchymal stem cell properties and senescence during bone aging. *Aging cell*, 17(1), <https://doi.org/10.1111/acer.12709>
- Mantovani, C., Raimondo, S., Haneef, M. S., Geuna, S., Terenghi, G., Shawcross, S. G., & Wiberg, M. (2012). Morphological, molecular and functional differences of adult bone marrow- and adipose-derived stem cells isolated from rats of different ages. *Experimental Cell Research*, 318(16), 2034–2048. <https://doi.org/10.1016/j.yexcr.2012.05.008>
- Martignoni, M., Groothuis, G. M., & de Kanter, R. (2006). Species differences between mouse, rat, dog, monkey and human CYP-mediated drug metabolism, inhibition and induction. *Expert Opinion on Drug Metabolism & Toxicology*, 2(6), 875–894. <https://doi.org/10.1517/17425255.2.6.875>
- Medeiros, T. C., Thomas, R. L., Ghillebert, R., & Graef, M. (2018). Autophagy balances mtDNA synthesis and degradation by DNA polymerase POLG during starvation. *Journal of Cell Biology*, 217(5), 1601–1611. <https://doi.org/10.1083/jcb.201801168>
- Oda, Y., Yoshimura, Y., Ohnishi, H., Tadokoro, M., Katsube, Y., Sasao, M., Kubo, Y., Hattori, K., Saito, S., Horimoto, K., Yuba, S., & Ohgushi, H. (2010). Induction of pluripotent stem cells from human third molar mesenchymal stromal cells. *Journal of Biological Chemistry*, 285(38), 29270–29278. <https://doi.org/10.1074/jbc.M109.055889>
- Pietilä, M., Palomäki, S., Lehtonen, S., Ritamo, I., Valmu, L., Nystedt, J., Laitinen, S., Leskelä, H. V., Sormunen, R., Pesälä, J., Nordström, K., Vepsäläinen, A., & Lehenkari, P. (2012). Mitochondrial function and energy metabolism in umbilical cord blood- and bone marrow-derived mesenchymal stem cells. *Stem Cells and Development*, 21(4), 575–588. <https://doi.org/10.1089/scd.2011.0023>
- Schimke, M. M., Marozin, S., & Lepperdinger, G. (2015). Patient-specific age: The other side of the coin in advanced mesenchymal stem cell therapy. *Frontiers in Physiology*, 6, 362. <https://doi.org/10.3389/fphys.2015.00362>
- Shipounova, I. N., Svinareva, D. A., Petrova, T. V., Lyamzaev, K. G., Chernyak, B. V., Drize, N. I., & Skulachev, V. P. (2010). Reactive oxygen species produced in mitochondria are involved in age-dependent changes of hematopoietic and mesenchymal progenitor cells in mice. A study with the novel mitochondria-targeted

- antioxidant SkQ1. *Mechanisms of Ageing and Development*, 131(6), 415–421. <https://doi.org/10.1016/j.mad.2010.06.003>
- Shyh-Chang, N., Daley, G. Q., & Cantley, L. C. (2013). Stem cell metabolism in tissue development and aging. *Development*, 140(12), 2535–2547. <https://doi.org/10.1242/dev.091777>
- Spees, J. L., Olson, S. D., Whitney, M. J., & Prockop, D. J. (2006). Mitochondrial transfer between cells can rescue aerobic respiration. *Proceedings of the National Academy of Sciences of the United States of America*, 103(5), 1283–1288. <https://doi.org/10.1073/pnas.0510511103>
- Stenderup, K., Justesen, J., Clausen, C., & Kassem, M. (2003). Aging is associated with decreased maximal life span and accelerated senescence of bone marrow stromal cells. *Bone*, 33(6), 919–926.
- Stolzing, A., Jones, E., McGonagle, D., & Scutt, A. (2008). Age-related changes in human bone marrow-derived mesenchymal stem cells: Consequences for cell therapies. *Mechanisms of Ageing and Development*, 129(3), 163–173. <https://doi.org/10.1016/j.mad.2007.12.002>
- Théry, C., Witwer, K. W., Aikawa, E., Alcaraz, M. J., Anderson, J. D., Andriantsitohaina, R., Antoniou, A., Arab, T., Archer, F., Atkin-Smith, G. K., Ayre, D. C., Bach, J. M., Bachurski, D., Baharvand, H., Balaj, L., Baldacchino, S., Bauer, N. N., Baxter, A. A., Bebawy, M., ... Jovanovic-Talisman, T. (2018). Minimal information for studies of extracellular vesicles 2018 (MISEV2018): A position statement of the International Society for Extracellular Vesicles and update of the MISEV2014 guidelines. *Journal of Extracellular Vesicles*, 7(1), 1535750. <https://doi.org/10.1080/20013078.2018.1535750>
- Torralba, D., Baixauli, F., & Sanchez-Madrid, F. (2016). Mitochondria know no boundaries: Mechanisms and functions of intercellular mitochondrial transfer. *Frontiers in Cell and Developmental Biology*, 4, 107. <https://doi.org/10.3389/fcell.2016.00107>
- Ucer, S., Iyer, S., Kim, H. N., Han, L., Rutlen, C., Allison, K., Thostenson, J. D., de Cabo, R., Jilka, R. L., O'Brien, C., Almeida, M., & Manolagas, S. C. (2017). The effects of aging and sex steroid deficiency on the murine skeleton are independent and mechanistically distinct. *Journal of Bone and Mineral Research*, 32(3), 560–574. <https://doi.org/10.1002/jbmr.3014>
- Wang, J., Zhu, P., Li, R., Ren, J., & Zhou, H. (2020). Fundc1-dependent mitophagy is obligatory to ischemic preconditioning-conferred renoprotection in ischemic AKI via suppression of Drp1-mediated mitochondrial fission. *Redox Biology*, 30, 101415. <https://doi.org/10.1016/j.redox.2019.101415>
- Wang, Y., Jasper, H., Toan, S., Muid, D., Chang, X., & Zhou, H. (2021). Mitophagy coordinates the mitochondrial unfolded protein response to attenuate inflammation-mediated myocardial injury. *Redox Biology*, 45, 102049. <https://doi.org/10.1016/j.redox.2021.102049>
- Yang, M., Wen, T., Chen, H., Deng, J., Yang, C., & Zhang, Z. (2018). Knockdown of insulin-like growth factor 1 exerts a protective effect on hypoxic injury of aged BM-MSCs: Role of autophagy. *Stem Cell Research & Therapy*, 9(1), 284. <https://doi.org/10.1186/s13287-018-1028-5>
- Yang, Y. K. (2018). Aging of mesenchymal stem cells: Implication in regenerative medicine. *Regen Ther*, 9, 120–122. <https://doi.org/10.1016/j.reth.2018.09.002>
- Zaim, M., Karaman, S., Cetin, G., & Isik, S. (2012). Donor age and long-term culture affect differentiation and proliferation of human bone marrow mesenchymal stem cells. *Annals of Hematology*, 91(8), 1175–1186. <https://doi.org/10.1007/s00277-012-1438-x>
- Zhang, H., Menzies, K. J., & Auwerx, J. (2018). The role of mitochondria in stem cell fate and aging. *Development*, 145(8), dev143420. <https://doi.org/10.1242/dev.143420>

**How to cite this article:** Barilani, M., Lovejoy, C., Piras, R., Abramov, A. Y., Lazzari, L., & Angelova, P. R. (2021). Age-related changes in the energy of human mesenchymal stem cells. *Journal of Cellular Physiology*, 1–15. <https://doi.org/10.1002/jcp.30638>